INTERVERTEBRAL DISC AND ENDPLATE CELL CHARACTERISATION HIGHLIGHTS ANNULUS FIBROSUS CELLS AS THE MOST PROMISING FOR TISSUE-SPECIFIC DISC DEGENERATION THERAPY

P. De Luca[1], M. Castagnetta[2], L. de Girolamo[1,*], S. Coco[3], M. Malacarne[4], E. Ragni[1], M. Viganò[1], G. Lugano[1], M. Brayda-Bruno[5], D. Coviello[4] and A. Colombini[1]

[1] IRCCS Istituto Ortopedico Galeazzi, Orthopaedic Biotechnology Lab, Milan, Italy
[2] Ospedali Galliera, Laboratorio di Istocompatibilità/IBMDR, Genoa, Italy
[3] IRCCS Ospedale Policlinico San Martino, Lung Cancer Unit, Genoa, Italy
[4] IRCCS Istituto Giannina Gaslini, Laboratorio di Genetica Umana, Genoa, Italy
[5] IRCCS Istituto Ortopedico Galeazzi, Scoliosis Unit, Department of Orthopaedics and Traumatology-Spine Surgery III, Milan, Italy

Abstract

Degenerative processes of the intervertebral disc (IVD) and cartilaginous endplate lead to chronic spine pathologies. Several studies speculated on the intrinsic regenerative capacity of degenerated IVD related to the presence of local mesenchymal progenitors. However, a complete characterisation of the resident IVD cell populations, particularly that isolated from the endplate, is lacking. The purpose of the present study was to characterise the gene expression profiles of human nucleus pulposus (NPCs), annulus fibrosus (AFCs) and endplate (EPCs) cells, setting the basis for future studies aimed at identifying the most promising cells for regenerative purposes.

Cells isolated from NP, AF and EP were analysed after *in vitro* expansion for their stemness ability, immunophenotype and gene profiles by large-scale microarray analysis.

The three cell populations shared a similar clonogenic, adipogenic and osteogenic potential, as well as an immunophenotype with a pattern resembling that of mesenchymal stem cells. NPCs maintained the greatest chondrogenic potential and shared with EPCs the loss of proliferation capability during expansion. The largest number of selectively highly expressed stemness, chondrogenic/tissue-specific and surface genes was found in AFCs, thus representing the most promising source of tissue-specific expanded cells for the treatment of IVD degeneration.

Keywords: Intervertebral disc, nucleus pulposus, annulus fibrosus, endplate, phenotype, microarray.

***Address for correspondence**: Laura de Girolamo, via Riccardo Galeazzi 4, 20161 Milano, Italy.
Telephone number: +39 0266214059 Email: laura.degirolamo@grupposandonato.it

List of Abbreviations

AF	annulus fibrosus
AFCs	AF cells
A2M	alpha-2-macroglobulin
ALDH1A3	aldehyde dehydrogenase 1 family member A3
ANKRD1	ankyrin repeat domain 1
BMPR1B	bone morphogenetic protein receptor type 1B
BST2	bone marrow stromal cell antigen 2
C5AR1	complement C5a receptor 1
CCL26	C-C motif chemokine ligand 26
CD	cluster of differentiation
CFU	colony-forming unit
CFU-F	CFU-fibroblast
CEBPA	CCAAT enhancer binding protein alpha
CHST6	carbohydrate sulphotransferase 6
CLDN11	claudin 11
CNMD	chondromodulin
COMP	cartilage oligomeric matrix protein
CXCR2	C-X-C motif chemokine receptor 2
DT	doubling time
DSC2	desmocollin 2
EDTA	ethylenediaminetetraacetic acid

EP	endplate
EPCs	EP cells
ERG	ETS transcription factor ERG
FAM20A	FAM20A golgi associated secretory pathway pseudokinase
FBS	foetal bovine serum
Fc	fold change
FGF18	fibroblast growth factor 18
FITC	fluorescein isothiocyanate
GAGs	glycosaminoglycans
GALNT3	polypeptide N-acetylgalactosaminyltransferase 3
GLDC	glycine decarboxylase
GPC3	glypican 3
HEPES	4-(2-hydroxyethyl)-1-piperazineethanesulphonic acid
HG-DMEM	high-glucose Dulbecco's modified Eagle medium
HHIP	hedgehog interacting protein
HLA-DRA	major histocompatibility complex, class II, DR alpha
IGFBP5	insulin-like growth factor binding protein 5
IVD	intervertebral disc
KRT14	keratin 14
KRT19	keratin 19
MSCs	mesenchymal stem cells
NANOG	nanog homeobox
NCAM1	neural cell adhesion molecule 1
NOX4	NADPH oxidase 4
NP	nucleus pulposus
NPCs	NP cells
NPR1	natriuretic peptide receptor 1
OCT4	organic cation/carnitine transporter 4
PDGFRL	platelet-derived growth factor receptor like
PE	phycoerythrin
PENK	preproenkephalin
POU5F1	POU class 5 homeobox 1
PTGIS	prostaglandin I2 synthase
RAI2	retinoic-acid-induced 2
RETN	resistin
RIN	RNA integrity number
ROR2	receptor tyrosine-kinase-like orphan receptor 2
SD	standard deviation
SERPINB2	serpin family B member 2
SFRP2	secreted frizzled-related protein 2
SORBS1	sorbin and SH3 domain containing 1
SOX2	SRY-box transcription factor 2
SPARC	secreted protein acidic and cysteine rich
SYT4	synaptotagmin 4
TBP	TATA-box binding protein
TBX2	T-box transcription factor 2
TEK	TEK receptor tyrosine kinase
TERT	telomerase reverse transcriptase
TMEM71	transmembrane protein 71
TP63	tumour protein p63
VCAM1	vascular cell adhesion molecule 1
YWHAZ	tyrosine 3-monooxygenase/ tryptophan 5-monooxygenase activation protein zeta

Introduction

The IVD is a complex avascular fibrocartilaginous structure composed of the gelatinous NP encapsulated in the AF (Colombini *et al.*, 2008). Between the disc and upper and lower vertebral bodies there is the interposition of the cartilaginous EP (Nguyen *et al.*, 2012). Each of these anatomical compartments has a peculiar matrix structure and cell populations with exclusive phenotypes and functions (Pattappa *et al.*, 2012). The degenerative processes of IVD and EP lead to chronical spine pathologies causing low-back pain and patient's disability. In particular, the nutrient supply to disc cells occurs by diffusion from the EPs; therefore, their calcification and/or subchondral bone sclerosis contribute to IVD degeneration (Urban *et al.*, 2004). The loss of disc height, mainly caused by cell death and proteoglycan degradation, results in decreased fluid-binding ability and reduction of IVD mechanical properties (Colombini *et al.*, 2008).

Several studies have speculated on the intrinsic regenerative capacity of degenerated IVD related to the presence of local mesenchymal progenitors (Blanco *et al.*, 2010; Brisby *et al.*, 2013; Brown *et al.*, 2018; Gruber *et al.*, 2016; Huang *et al.*, 2012) or NPCs with a notochordal-like phenotype (Rodrigues-Pinto *et al.*, 2018). Nevertheless, the IVD degeneration is difficult to counteract for many reasons – including the small number of resident cells and their inability to prevent efficiently the tissue damage produced by the chronic catabolic and inflammatory environment in which they reside. Regenerative medicine would provide different tools for the treatment of degenerative disc disease by means of tissue-specific cell therapy; therefore, a complete characterisation of the resident IVD cell populations would allow focusing on those with the highest regenerative capability. To achieve good results, cell expansion is required because only few cells are initially isolated from pathological tissues and because a range of 1-120 million cells (MSCs or NPCs) per disc has been used in clinical trials (Schol and Sakai, 2019). CFU ability has been also reported as a parameter associated with a good clinical outcome for the treatment of IVD degeneration (Pettine *et al.*, 2016; Pettine *et al.*, 2015; Pettine *et al.*, 2017). A recent study of osteoarthritic human articular cartilage-derived cells has observed an enhanced clonogenic ability and sustained expression of stemness markers in cells throughout *in vitro* expansion, suggesting that this heterogeneous cell population conserves (or even expands) a chondrogenic progenitor pool of cells over time (De Luca *et al.*, 2019). Therefore, it would

be interesting to confirm these results also for NPCs, AFCs and EPCs.

Although several studies have characterised IVD cells, to date only preliminary studies have been conducted to fingerprint the molecular signature of IVD cell subtypes. However, there are still many controversies, especially about the influence of age and pathological status. A subset of notochord-specific markers was identified in human NPCs (Rodrigues-Pinto *et al.*, 2018). Moreover, the expression of keratins, already identified in human embryonic and foetal spine as well as in human unexpanded, freshly isolated, adult NPCs obtained from degenerated IVDs, demonstrates that this population contains a notochord-derived cell subpopulation (Rodrigues-Pinto *et al.*, 2016; Rutges *et al.*, 2010). Particularly, higher levels of *KRT19* – with an age-related decrease and detection only in donors younger than 54 years – as well as of *NCAM1*, *A2M* and *DSC2* are noted in NPCs when compared to AFCs, whilst *COMP* and *GPC3* expression is higher in AFCs (Rutges *et al.*, 2010). Another marker of a progenitor population in human-expanded NPCs that decreases with age and IVD degeneration degree is *TEK* (Sakai *et al.*, 2012). Nevertheless, since *TEK* is also expressed in AFCs, it is not specific for NPCs (Schubert *et al.*, 2018). Indeed, a larger inter-subject similarity was found when comparing the transcriptome profile of AFCs and NPCs; a higher expression of only some surface markers was observed in NPCs with respect to AFCs (Power *et al.*, 2011). Furthermore, 11 out of 47,000 transcribed genes analysed were identified as differentially expressed in NPCs or AFCs derived from cervical discs (Schubert *et al.*, 2018).

Despite their involvement in the pathogenesis of IVD degeneration (Jackson *et al.*, 2011; Urban *et al.*, 2004), few studies have characterised EPCs. In this population, after progenitor cell selection, the stem-cell-related genes *OCT4*, *NANOG* and *SOX2* are expressed (Huang *et al.*, 2012). The purpose of the present study was to characterise the human-expanded NPC, AFC and EPC stemness potential, immunophenotype and gene expression profiles by large-scale microarray analysis, with particular emphasis on the expression of stemness, chondrogenic, surface and senescence markers. The identification of the cells with the greatest stemness and trophic potential as well as of markers characteristic of a single cell population will allow the selection of the most promising tissue-specific cells for the treatment of IVD degeneration. Finally, differently from the great interest in the restoration of NP, few studies have focused on the repair of the AF (Sakai and Grad, 2015) or EP (Bendtsen *et al.*, 2011) although their integrity is fundamental for disc health (Bendtsen *et al.*, 2016). For this reason, thoroughly assessing the features and therapeutic potential of the cells derived from each of these anatomical tissues will be necessary.

Materials and Methods

Human tissue harvesting

The present study was approved by the Institutional Review Board (GenVDisc Version 1, 20 November 2015 protocol for use of waste biological material) and specimens were collected after receiving patient informed consent. NP, AF and EP from lumbar IVD of 8 patients (mean age 51.9 ± 6.9 years; 4 males and 4 females) affected by discopathy, Pfirrmann grade III-IV, were harvested during discectomy through an accurate macroscopic dissection performed by an experienced surgeon.

Cell isolation and expansion

NPCs, AFCs and EPCs were isolated by enzymatic digestion as previously described (Colombini *et al.*, 2015; Lopa *et al.*, 2016). NPCs, AFCs and EPCs were cultured in a control medium consisting of 4.5 mg/mL HG-DMEM (Life Technologies) supplemented with 10 % FBS (Lonza), 0.29 mg/mL L-glutamine, 100 U/mL penicillin, 100 µg/mL streptomycin, 10 mM HEPES and 1 mM sodium pyruvate (all from Life Technologies). For all cell types, the seeding density was 5×10^3 cells/cm^2.

Cell DT

Disc-cell DT was calculated from passages 1 to 3. Cells were plated at a density of 5×10^3 cells/cm^2 in control medium. Fresh medium was supplied every 3 d and cells were split at 80-90 % confluence using trypsin/EDTA (0.5 % trypsin/0.2 % EDTA; Sigma-Aldrich). DT was calculated using the equation

$$DT = CT/\ln(Nf - Ni)/ln2$$

where *CT* is the cell culture time (h), *Nf* is the final number of cells and *Ni* is the initial number of cells.

Clonogenic ability

A CFU-F assay was performed to assess the cell clonogenic ability (Lopa *et al.*, 2014) at P1 and P3. Cells were plated at different low densities (range: 48-12 cells/cm^2) and cultured in control medium with 20 % FBS. After 14 d, cells were fixed in 10 % neutral-buffered formalin and stained using Gram's crystal violet (Sigma-Aldrich). CFU-F frequency was established by expressing the number of colonies as a percentage relative to the number of seeded cells.

Multi-lineage differentiation

Previously validated adipogenic or osteogenic differentiation protocols (de Girolamo *et al.*, 2009) were used on cells at P1 and P3. Lipid vacuoles were quantified by oil red O staining and absorbance was read at 490 nm (Perkin Elmer Victor X3 microplate reader). Alizarin red S staining was performed to assess calcified matrix deposition (Sigma-Aldrich) and absorbance was read at 570 nm.

Chondrogenic differentiation was obtained by centrifugation of 4 × 10^5 cells (2 min at 232 ×*g*) at P1 and P3. Then, the pellets were maintained for 28 d in chondrogenic medium as already reported (Colombini *et al.*, 2012). Pellets were fixed in 10 % neutral-buffered formalin, embedded in paraffin-wax, sectioned at 4 µm thickness and stained using alcian blue (Sigma-Aldrich) to evaluate GAG deposition. GAG quantification was performed using dimethylmethylene blue (Sigma-Aldrich) and absorbance was read at 500 nm.

Immunophenotype

Flow cytometry analyses were conducted on 2.5 × 10^5 expanded cells (P3) incubated with anti-human primary monoclonal antibodies: CD34-biotinylated, CD44-FITC, CD45-FITC, CD105-biotinylated, CD166-FITC (all from Ancell Corporation, Bayport, MN, USA), CD90-FITC and CD73-PE (Miltenyi Biotec) and CD151 (R&D Systems) (De Luca *et al.*, 2019). Cells stained with biotinylated antibodies were incubated with streptavidin-PE (Ancell Corporation), whereas samples stained with anti-CD151 primary antibody were incubated with a FITC-conjugated goat anti-mouse secondary antibody (Ancell Corporation). Background fluorescence was established by unstained controls. A minimum of 10,000 events were acquired using a FACSCalibur flow cytometer (BD Biosciences) and analysed using CellQuest software (BD Biosciences).

RNA isolation and quality assessment

RNA was isolated from lysates of cell at P3 using the RNeasy Plus Mini Kit (Qiagen). RNase-Free DNase Set (Qiagen) was used for residual genomic DNA digestion and the isolated RNA was quantified and its purity checked spectrophotometrically (Nanodrop, Thermo Fisher Scientific). Agilent RNA ScreenTape System (Agilent Technologies) was used to evaluate the RIN, where values range from 10 (intact RNA) to 1 (totally degraded RNA) (Schroeder *et al.*, 2006) (Fig. 1).

Gene expression microarray

All reagents, instruments and software when not specified were purchased from Agilent Technologies.

The One-Color RNA Spike-In Kit was used to prepare a spike mix to add to the samples, useful to assess the correct annealing of 10 optimised positive control transcripts to the complementary probes of the array, evaluating also the auto- and cross-hybridisation.

RNA (100 ng) of 4 pooled donors for each cell type at P3 was labelled and amplified using a Low Input Quick Amp Labeling Kit, one-colour, to obtain cRNA. The obtained cRNA was purified using an RNeasy Plus Mini Kit (Qiagen) and used with the Gene Expression Hybridization Kit for the microarray hybridisation. To evaluate the gene expression profile of interest, a suitable Agilent Technologies algorithm was used (Web ref. 1). The custom gene expression microarray allowed to analyse a maximum of 3,000 genes considering a minimum of 5 replicates for each gene. Gene symbol and NM of the analysed genes, divided into housekeeping, chondrogenic/IVD/growth factors, surface, stemness and senescence, are reported in Supplementary Table 1. After washing, the microarray slide was scanned using SureScan Microarray Scanner and, to obtain a high-resolution image of the fluorescence values for each probe, the data were extracted by Feature Extraction v.12.0 software. Data analysis was performed by means of Genespring GX software and an Fc over or under an arbitrary cut-off of 2 was considered of interest.

Only up- or down-regulated genes (Fc ≥ + 2 or ≤ − 2) in the different cell populations were described. Gene ontology analyses were performed using Panther, PubMed, QuickGO and GeneCards databases.

Gene expression analysis and microarray validation

The expression of the pluripotent stem cell markers *NANOG* (Hs04260366_g1) and *POU5F1* (Hs04260367_gh), already extensively used to characterise IVD cells (Lyu *et al.*, 2019), was evaluated at P1 and P3.

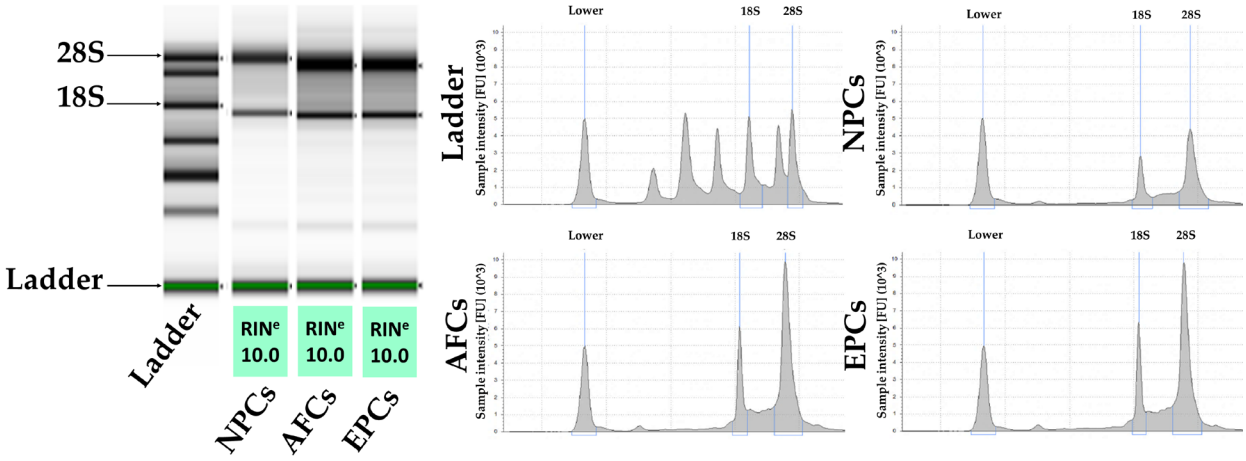

Fig. 1. Quality assessment of isolated RNA from a pool of NPCs, AFCs and EPCs obtained from 4 donors. FU: fluorescence units.

Table 1. Gene symbols and TaqMan® probe codes of validated genes.

Gene	Assay
TBP	Hs00427620_m1
YWHAZ	Hs01122445_g1
ANKRD1	Hs00173317_m1
CLDN11	Hs00194440_m1
FGF18	Hs00818572_m1
IGFBP5	Hs00181213_m1
KRT14	Hs00265033_m1
KRT19	Hs00761767_s1
SYT4	Hs01086433_m1
C5AR1	Hs00383718_m1
RETN	Hs00220767_m1
CXCR2	Hs00174304_m1
ERG	Hs01554629_m1
FAM20A	Hs01034073_m1
HHIP	Hs00368450_m1
TEK	Hs00945150_m1

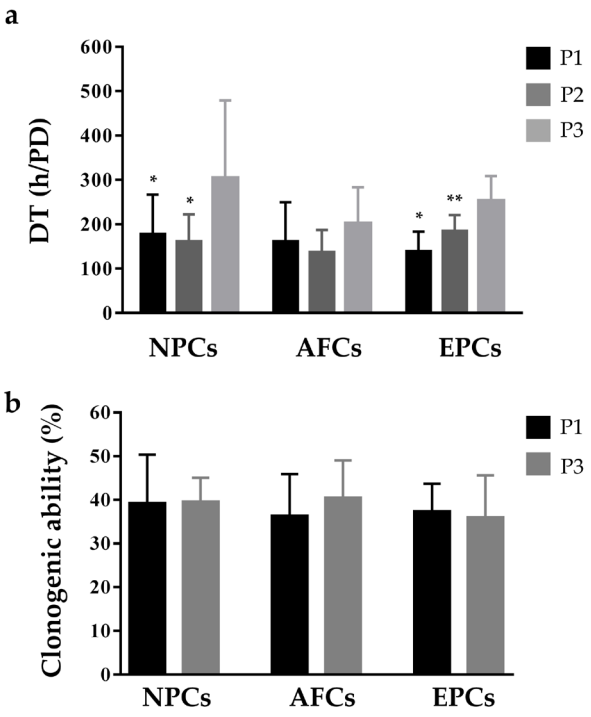

Fig. 2. DT of IVD cells at P1 and P3. (**a**) Disc cell DT from passages 1 to 3. * $p < 0.05$, ** $p < 0.01$ *vs.* P3. PD: population doubling. (**b**) Clonogenic ability; $n = 8$ donors.

14 genes of which 3 for NPCs (*C5AR1*, *CLDN11*, *SYT4*), 9 for AFCs (*ANKRD1*, *ERG*, *FAM20A*, *FGF18*, *HHIP*, *IGFBP5*, *KRT14*, *KRT19*, *TEK*) and 2 for EPCs (*CXCR2*, *RETN*) were validated in cells derived from the 3 donors used for microarray gene expression analysis and in cells derived from another patient of the 8 enrolled in the study.

Table 2. Immunophenotype of IVD cells. Mean of percentage ± SD of cells positive for typical mesenchymal (green) and haematopoietic (red) markers; $n = 6$ donors.

	NPCs	AFCs	EPCs
CD34	2.7 ± 2.4	2.7 ± 2.0	3.3 ± 2.3
CD45	2.3 ± 1.9	2.7 ± 1.4	3.9 ± 2.1
CD146	5.8 ± 2.9	3.3 ± 1.4	5.2 ± 2.4
CD44	98.3 ± 3.0	98.5 ± 1.6	96.4 ± 4.9
CD73	99.6 ± 0.4	99.5 ± 0.7	99.7 ± 0.2
CD90	94.4 ± 2.9	94.2 ± 5.7	96.4 ± 3.5
CD105	87.0 ± 14.4	94.0 ± 7.3	91.4 ± 5.3
CD151	95.0 ± 4	87.9 ± 16.4	88.9 ± 8.8
CD166	65.1 ± 20.9	73.0 ± 19.1	68.8 ± 26.6

RNA was isolated from disc cells using the RNeasy Plus Mini Kit, quantified spectrophotometrically (NanoDrop, Thermo Fisher Scientific), reverse-transcribed using the iScript cDNA Synthesis Kit (Bio-Rad Laboratories) and gene expression was evaluated by real-time PCR (StepOne Plus, Life Technologies) using TaqMan® Gene Expression Master Mix and TaqMan® Gene Expression Assays (Life Technologies).

TBP and *YWHAZ* were evaluated as housekeeping genes. *TBP* was selected for its higher stability, as observed in a previously published validation (Lopa *et al.*, 2016) and in the present study. Data are expressed according to the ΔΔCt method. TaqMan® Gene Expression Assays used for validation are reported in Table 1.

Statistical analysis

Data are expressed as mean ± SD. Kolmogorov-Smirnov normality test was used to assess normal data distribution, Student's *t*-test for normally distributed data and Wilcoxon test in the absence of a normal distribution (GraphPad Prism v5.00). Level of significance was set at * $p < 0.05$, ** $p < 0.01$ and *** $p < 0.001$.

Results

NPCs, AFCs and EPCs shared clonogenic behaviour and immunophenotype, while showed different proliferative and chondrogenic potential

NPCs and EPCs shared an increase in DT during culture expansion (P2 *vs.* P3 $p < 0.05$ and $p < 0.01$, respectively, and P1 *vs.* P3 $p < 0.05$ for both cell types), whereas AFCs did not show any change (Fig. 2**a**). The clonogenic ability was similar for all the IVD cells at P1 and maintained until P3 (Fig. 2**b**). All three cell populations displayed a similar immunophenotype. They were negative for CD34, CD45, CD146 and positive for CD44, CD73, CD90, CD105, CD151 and CD166 (Table 2).

All disc cells displayed osteogenic (Fig. 3**a**) and chondrogenic (Fig. 3**b**) capability. From P1 to P3

AFCs and EPCs showed a loss of their chondrogenic differentiation potential, whereas NPCs showed a stable chondrogenic capability with passages. No adipogenic differentiation was observed. *POU5F1* and *NANOG* were expressed by all the analysed disc cells, whereas AFCs and EPCs showed a decrease of their expression from P1 to P3 (data not shown).

Gene expression microarray in expanded cells

Stemness genes

AFCs showed the largest number of highly expressed stemness genes, followed by EPCs and NPCs (Fig. 4a, Supplementary Table 2). In particular *ANO2*, *BST2*, *CCL26*, *CEBPA*, *CHST6*, *CNMD*, *ERG*, *FAM20A*, *GALNT3*, *GLDC*, *HHIP*, *NPR1*, *PDGFRL*, *PTGIS*, *RAI2*, *ROR2*, *SFRP2*, *SORBS1* and *TEK* were more expressed in AFCs in comparison to both NPCs and EPCs. Moreover, validation of gene expression confirmed the higher expression of *ERG*, *FAM20A* and *HHIP* in AFCs in comparison to the other two cell populations (Fig. 5). No gene was more expressed selectively in NPCs and only *CXCR2* was more expressed in EPCs with respect to the other two populations, although after validation this gene was undetected in all samples. Table 3 reports the molecular functions of these genes, which mainly are related to catalytic and binding activity.

Concerning the similarities between cell populations, AFCs and EPCs shared 53 genes more highly expressed than in NPCs, whereas only 9 genes had a higher expression in NPCs and EPCs than in AFCs. NPCs and AFCs shared no genes with a higher expression than in EPCs. In Fig. 4**b**, genes with a higher expression in one disc-cell population in comparison to another are shown. AFCs showed upregulation of 47 and 5 stemness genes in comparison to NPCs and EPCs, respectively; NPCs presented 22 and 8 genes with higher expression than AFCs and EPCs, respectively; EPCs had 18 and 2 genes with higher expression than AFCs and NPCs, respectively.

Surface marker genes

AFCs and EPCs shared 22 surface-related genes with a higher expression in comparison to NPCs, while EPCs shared only 2 genes with NPCs with a higher expression than in AFCs (Fig. 6**a**, Supplementary Table 2). Among these markers, *CD74* and *HLA-DRA* were more expressed in AFCs, *C5AR1* in NPCs and *VCAM1* and *RETN* in EPCs than in the other two cell populations. After validation, *C5AR1* and *RETN* resulted undetected. The molecular functions of these genes are shown in Table 4. Genes with higher expression in one disc-cell population in comparison to another are shown in Fig. 6**b**.

Chondrogenic, IVD- and growth-factor-related genes

AFCs and EPCs shared 22 genes more expressed than in NPCs, while EPCs and NPCs shared only 7 genes in comparison to AFCs (Fig. 7**a**, Supplementary

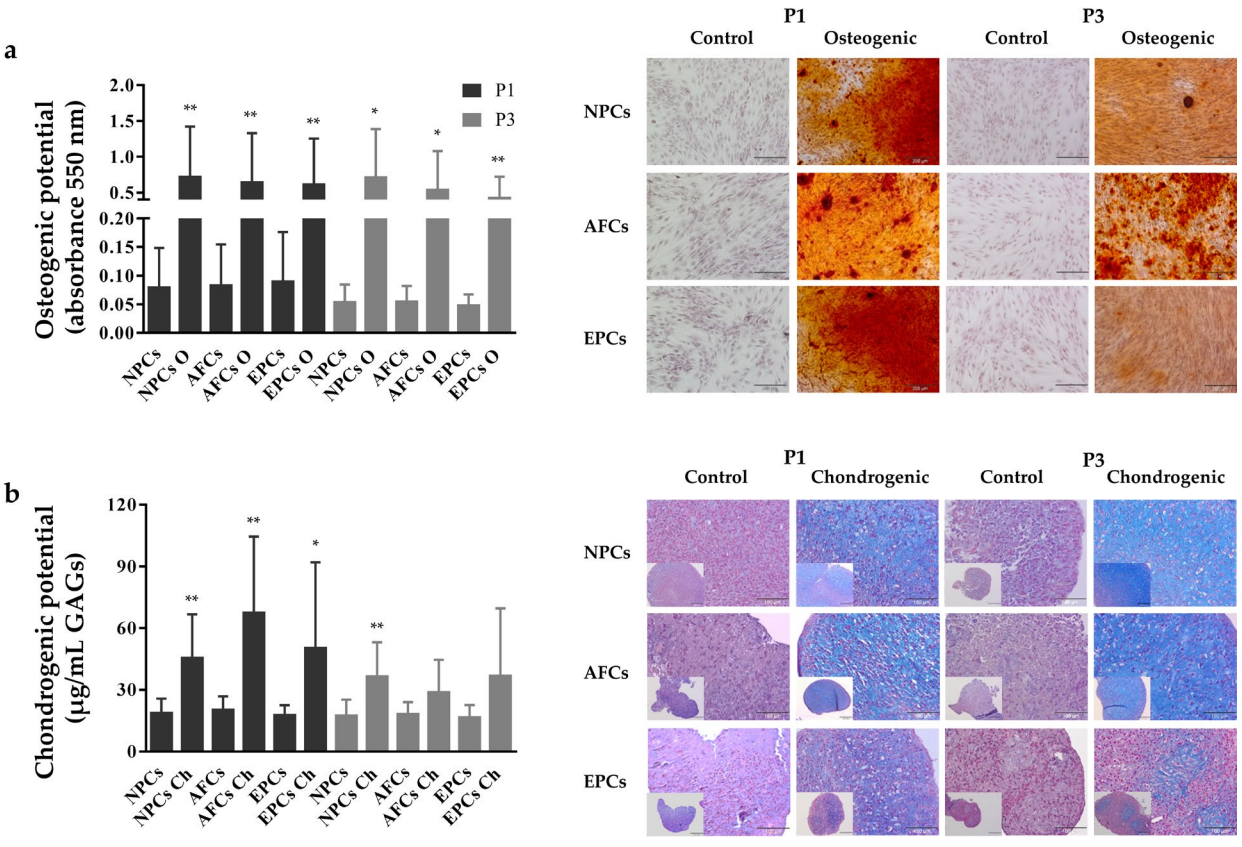

Fig. 3. Multi-lineage differentiation of IVD cells at P1 and P3. (**a**) Osteogenic and (**b**) chondrogenic cell differentiation. Scale bars: 200 µm. Scale bars of the bigger chondrogenic images: 100 µm. * $p < 0.05$, ** $p < 0.01$ of NPCs, AFCs or EPCs differentiated *vs.* control; $n = 8$ donors. Ch = chondrogenic; O = osteogenic.

Table 3. Protein class and molecular function of stemness-related genes. Molecular function legend: a = binding function, b = transcription regulator activity, c = catalytic activity, d = molecular function regulator, e = molecular transducer activity, f = developmental function, n.d. = not defined, / = no differences between cell populations. Higher expressed genes in AFCs (red) and EPCs (blue). *n* = pool of 4 donors.

Gene	Protein class	Molecular function	Fc AFCs *vs.* NPCs	Fc AFCs *vs.* EPCs	Fc EPCs *vs.* NPCs
ANO2	Transmembrane protein 16B	n.d.	3.4	3.4	/
BST2	n.d.	a, c, d	5.1	4.4	/
CCL26	Chemokine	a, c, d, e	2.5	3.6	/
CEBPA	Basic leucine zipper transcription factor, nucleic acid binding	a, b	2.4	2.4	/
CHST6	Sulphotransferase	c	3.1	6.1	/
CNMD	Glycosylated transmembrane protein	f	2.8	2.2	/
CXCR2	C-X-C motif chemokine receptor 2	c, e	2.4	− 2.9	2.4
ERG	Nucleic acid binding, signaling molecule transcription factor	b	2.9	8.0	− 2.7
FAM20A	Allosteric activator of the Golgi Serine/threonine protein kinase FAM20C	c	17.9	14.6	/
GALNT3	Calcium ion binding and transferase activity	c	2.2	3.0	/
GLDC	Dehydrogenase	a, c	2.1	4.2	/
HHIP	Quinone binding and hedgehog family protein binding	a	15.2	5.8	/
NPR1	Adenylate/guanylate cyclase	a, c, e	2.2	2.2	/
PDGFRL	Tyrosine protein kinase receptor	c	2.4	2.7	/
PTGIS	Endoplasmic reticulum membrane protein	a, c	5.5	5.1	/
RAI2	n.d.	a	4.0	3.6	/
ROR2	Transmembrane protein	a, c	2.1	3.2	/
SFRP2	G-protein-coupled receptor, protease inhibitor, signaling molecule	a, e	3.6	6.0	/
SORBS1	Protein kinase binding, cytoskeletal protein binding	a	2.2	2.8	/
TEK	Cell-surface receptor	c	3.0	3.5	3.5

Table 2). Among these genes, *ANKRD1*, *BMPR1B*, *CSF1R*, *FGF18*, *IGFBP5*, *KRT14*, *KRT19*, *PENK*, *REEP1* and *TMEM71* were more expressed in AFCs in comparison to the other two populations. After validation, these results were confirmed in 3 patients out of 4 for *ANKRD1* and *KRT14*, whereas *FGF18*, *IGFBP5* and *KRT19* were confirmed in all patients (Fig. 5). Only *CLDN11* and *SYT4* were more expressed in NPCs in comparison to the other two cell populations and this result was confirmed in 3 patients out of 4. In Table 5 are shown the molecular functions of these genes.

In Fig. 7**b** genes with a higher expression in one disc-cell population in comparison to another are shown. In particular, NPCs showed a higher expression of 11 genes in comparison to AFCs. An upregulation of 5 genes in comparison to NPCs and of 3 genes in comparison to EPCs was observed in AFCs. EPCs showed higher expression of 1 and 11 genes in comparison to NPCs and AFCs, respectively.

Senescence/telomere-related genes

Analysing the genes related to senescence and telomere markers, AFCs showed the highest value of *TP63* when compared to both NPCs and EPCs. More in general, NPCs and EPCs showed a higher expression of *TBX2* and *TERT* in comparison to AFCs. *SPARC* upregulation was observed in EPCs in comparison to AFCs. An upregulation of *NOX4* and *SERPINB2* was observed in AFCs and EPCs in comparison to NPCs. *ALDH1A3* upregulation was observed in AFCs in comparison to EPCs. In Supplementary Table 2, fold change of up- or down-regulated senescence/telomere-related genes are shown.

Discussion

The present study allowed the deep characterisation of the different cell populations of the human IVD.

Fig. 4a. Stemness genes expression in IVD cells. Gene array showing only the differently expressed genes between cell populations. Heat map was created using a two-colour scale from red (highest value) to yellow (lowest value); *n* = pool of 4 donors.

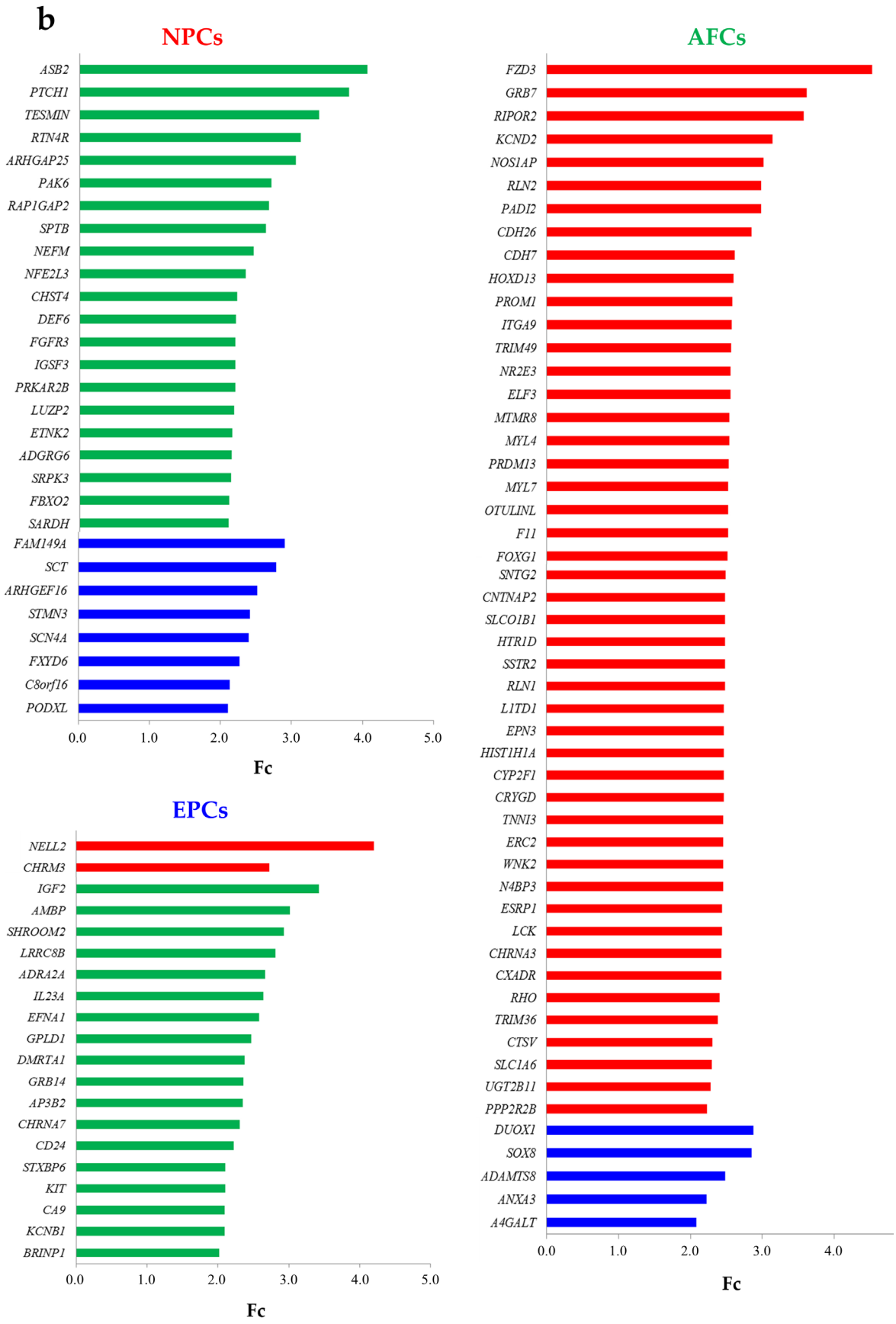

Fig. 4b. Stemness genes expression in IVD cells. Higher expressed genes in one single disc-cell population respect to another one. NPCs (red), AFCs (green) and EPCs (blue); *n* = pool of 4 donors.

The validated markers obtained could be used to identify AFCs in the presence of a mixed biological material consisting of tissue contaminated by the NP, if considering surgical waste samples from discectomy as a potential reservoir of cells to be exploited for cell-based treatment of IVD degeneration. In fact, the higher expression of stemness and chondrogenic genes in expanded AFCs with respect to the other two cell populations would suggest that these cells could be the preferential focus of future approaches of tissue-specific cell therapies for IVD degeneration. In addition, as far as it can be ascertained, the present was the first study in which EPCs, highly involved in IVD homeostasis, were compared with the other two most studied IVD cell types.

Despite the morphological differences in the structural organisation of the different anatomical portions of the IVD to which they belong, NPCs, AFCs and EPCs showed common proliferative, clonogenic, multi-differentiation characteristics and immunophenotype, which were maintained during culture. Differences were observed only in terms of loss of proliferative potential by NPCs and EPCs and of chondrogenic potential and pluripotent stem cell gene expression (*POU5F1* and *NANOG*) by AFCs and EPCs at P3. The surface marker layout after expansion indicated a typical MSC-like immunophenotype (Dominici *et al.*, 2006) of IVD cells and the positivity for CD44, CD73, CD90, CD105 and CD166 was consistent with what has already been observed in IVD cells (Blanco *et al.*, 2010; Brisby *et al.*, 2013; Liu *et al.*, 2011; Wang *et al.*, 2014). Furthermore, although they have an MSC-like immunophenotype, IVD cells do not share a perivascular origin given the lack of CD146 expression. To reinforce the MSC-like phenotype of the analysed disc cells, CD151 also showed a high expression already previously observed in articular chondroprogenitor cells (De Luca *et al.*, 2019) and MSCs (Lee *et al.*, 2009).

A group of stemness, surface and chondrogenic genes was found as selectively upregulated in expanded single-cell populations. After validation, the stemness genes *ERG*, *FAM20A*, *HHIP* and the chondrogenic *FGF18*, *IGFBP5* and *KRT19* were confirmed as being selective for AFCs in all patients, suggesting that these genes can be exploited as specific cell population markers. Differently, the chondrogenic genes *ANKRD1* and *KRT14* for AFCs and *CLDN11* and *SYT4* for NPCs after validation were confirmed in 3 out of 4 patients, suggesting a more donor-dependent result. Thus, they cannot be considered reliable as single disc-cell population markers.

The stemness marker *CXCR2* and the surface markers *C5AR1* and *RETN* were not confirmed after validation by real-time PCR. It is possible to ascribe this result to their lower expression and consequent inefficacious detection. For this reason, these markers should be not considered as being specific for a single IVD cell population. Consistently with the study's findings, other studies have shown that *NCAM1* and *A2M* are more expressed in NPCs in comparison to

Table 4. Protein class and molecular function of cell-surface-related genes. Molecular function legend: a = binding function, c = molecular function regulator, d = molecular transducer activity, e = hormone activity, / = no differences between cell populations. Higher expressed genes in NPCs (green), AFCs (red) and EPCs (blue). *n* = pool of 4 donors.

Gene	Protein class	Molecular function	Fc AFC *vs.* NPC	Fc AFC *vs.* EPC	Fc EPC *vs.* NPC
C5AR1	Protease inhibitor	a, c	− 3.6	/	− 2.2
CD74	Major histocompatibility complex, class II, DR alpha	c, d	2.9	2.3	/
HLA-DRA	Major histocompatibility complex, class II, DR alpha	c	7.5	3.8	/
RETN	Cysteine-rich secreted protein	e	/	− 4.75	3.9
VCAM1	Type I membrane protein	a	/	− 2.2	2.2

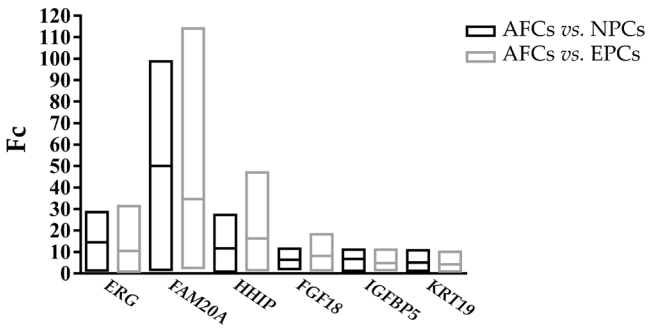

Fig. 5. Fc of genes validated by means of real-time PCR in cells obtained from the 3 single donors used for microarray gene expression analysis and from another patient of the 8 enrolled for the study Floating bars show line at mean, minimum and maximum Fc.

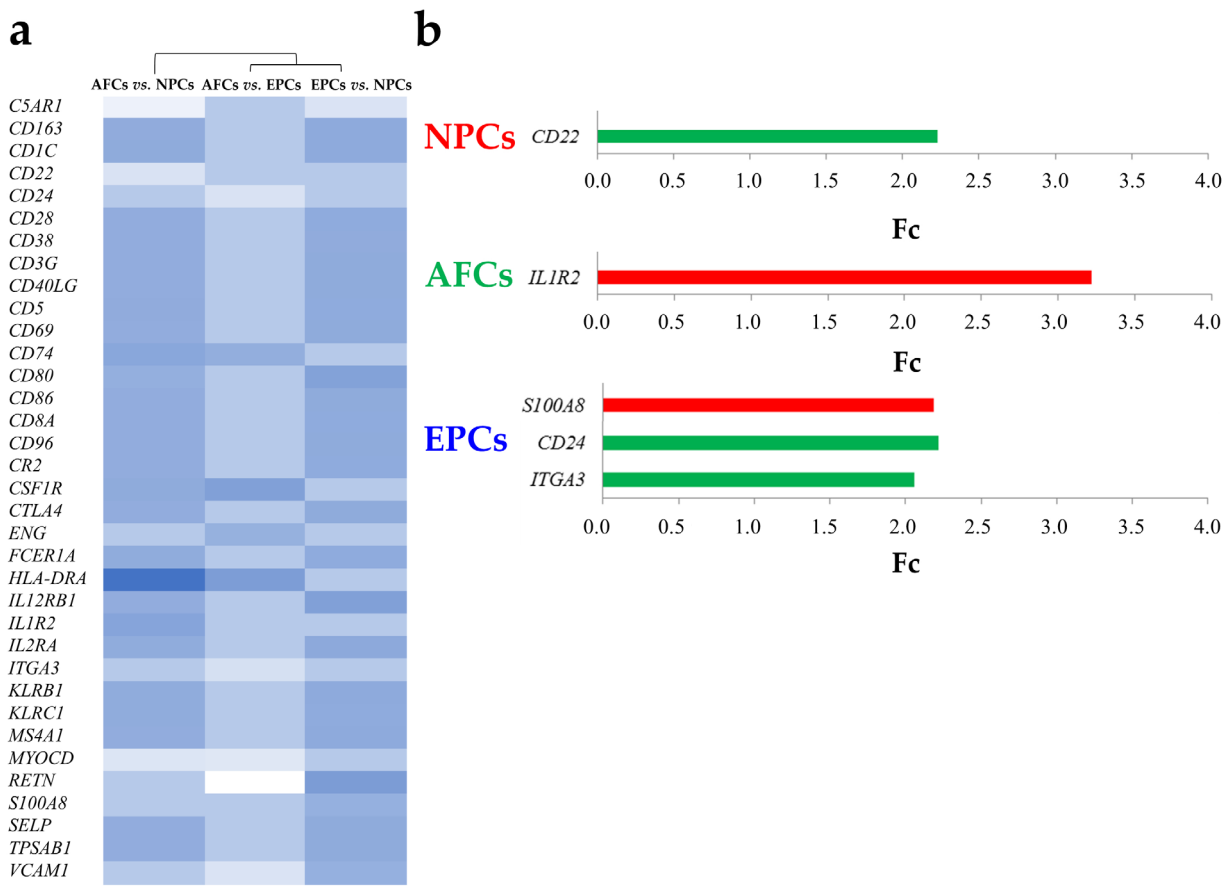

Fig. 6. Surface marker genes in IVD cells. (**a**) Gene array showing only the differently expressed genes between cell populations. Heat map was created using a two-colour scale from dark blue (highest value) to white (lowest value). (**b**) Higher expressed genes in one single disc-cell population respect to another. NPCs (red), AFCs (green) and EPCs (blue); *n* = pool of 4 donors.

Table 5. Protein class and molecular function of chondrogenic, IVD- and growth-factor-related genes. Molecular function legend: a = binding function, b = catalytic activity, c = molecular function regulator, d = molecular transducer activity and e = developmental function, n.d. = not defined, / = no differences between cell populations. Higher expressed genes in NPCs (green) and AFCs (red). *n* = pool of 4 donors.

Gene	Protein class	Molecular function	Fc AFC *vs.* NPC	Fc AFC *vs.* EPC	Fc EPC *vs.* NPC
ANKRD1	RNA polymerase II transcription factor binding	a	11.4	4	/
BMPR1B	Growth factor binding, transmembrane receptor protein	a, b	5.3	5.5	/
CLDN11	Transmembrane protein	d	− 4.2	/	− 3.5
CSF1R	Transmembrane receptor protein	b	2.2	4	/
FGF18	Growth factor	c	5.4	9.7	/
IGFBP5	Protease inhibitor	a	2.5	3.8	/
KRT14	Structural protein	a	8.7	11.2	/
KRT19	Structural protein	a	2.4	3	/
PENK	Neuropeptide	d	5	5.8	/
REEP1	Receptor, transporter	a, e	2.8	4	/
SYT4	Membrane trafficking regulatory protein	a	− 2.2	/	− 3
TMEM71	Transmembrane protein	n.d.	2.4	3.1	/

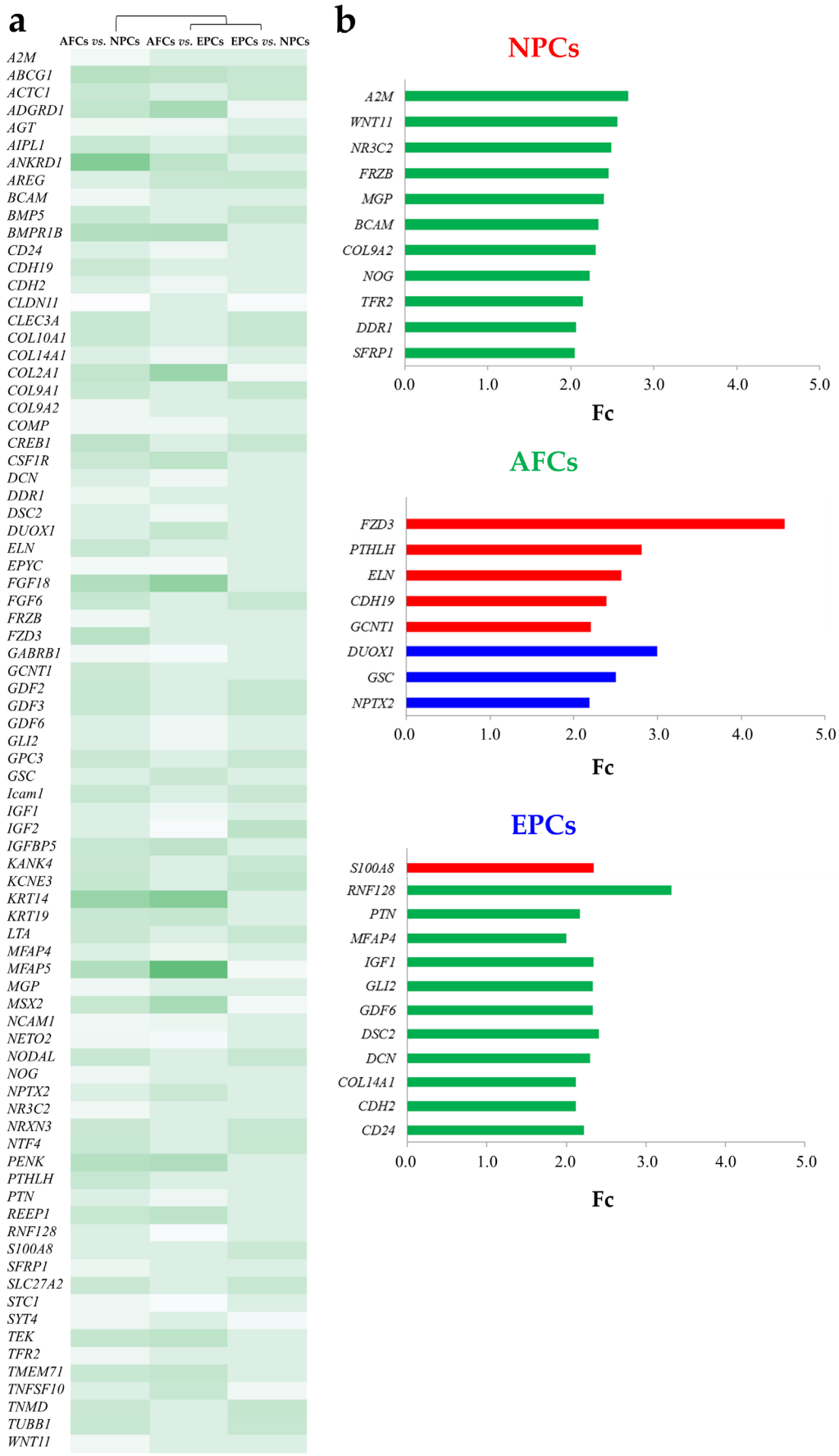

Fig. 7. Chondrogenic, trophic and growth-factor-related genes in IVD cells. (**a**) Gene array showing only the differently expressed genes between cell populations. Heat map was created using a two-colour scale from dark green (highest value) to white (lowest value). (**b**) Higher expressed genes in one single disc-cell population respect to another. NPCs (red), AFCs (green) and EPCs (blue); *n* = pool of 4 donors.

AFCs (Rutges *et al.*, 2010), while *GPC3* (Rutges *et al.*, 2010) and *TEK* (Schubert *et al.*, 2018) are more expressed in AFCs. In contrast, in the present study, *COMP* was more expressed in NPCs and not in AFCs (Rutges *et al.*, 2010) while the notochordal *KRT19* was more expressed in AFCs and not in NPCs, as previously reported (Rodrigues-Pinto *et al.*, 2016; Rutges *et al.*, 2010). These discrepancies can be ascribed to the use of expanded cells undergoing dedifferentiation in the present study, while in previously published works the expression of these genes was evaluated directly in tissue explants (Rutges *et al.*, 2010) or in embryonal discs (Rodrigues-Pinto *et al.*, 2016).

AFCs and EPCs shared a larger number of highly expressed stemness, surface-related, chondrogenic, trophic and growth-factor-related genes, mainly having catalytic and binding activity. In particular, AFCs showed the largest number of highly expressed genes related to stemness ability, followed by EPCs and NPCs. Another indicator of the possible capability of AFCs in terms of their therapeutic use was the higher expression of *TP63*, a key regulator of ageing and senescence (Keyes and Mills, 2006), in these cells in comparison to both NPCs and EPCs. At the same time, NPCs and EPCs showed a higher expression of *TBX2* and *TERT* than AFCs. Since the other analysed genes in the senescence pathway did not allow the establishment of whether there was a prevalence of pro- or anti-senescence processes in these IVD populations, further studies will be needed to better clarify if one of these population is less prone to senescence.

The main limitation of the study was that the microarray analysis was conducted on 4 pooled donors for each cell type. Nevertheless, the identified genes were validated in cells obtained from the 3 single donors used for microarray gene expression analysis and from another patient of the 8 enrolled in the study. Moreover, the study did not include a functional analysis, which could have further helped to identify AFCs as the most suitable disc cell population for regenerative purposes. Finally, since cell expansion may cause alterations of the phenotype and surface markers related to *in vitro* dedifferentiation, especially in cells having a more chondrogenic phenotype such as NPCs and EPCs, the present findings should be considered applicable only to monolayer-expanded cells. It would be interesting to compare the outcome of the present study to results obtained from cells directly isolated from the respective tissue region to study possible influences of sub-culturing the cells in monolayer.

Conclusions

The study provided a whole gene expression characterisation of expanded AFCs, NPCs and EPCs identifying also a panel of genes useful to detect AFCs in the presence of a mixed material consisting of an AF contaminated by an NP. In fact, due to a stemness and chondrogenic profile that resembles that of regenerative cells such as MSCs, AFCs appeared as the most promising source of tissue-specific expanded cells to be used in cell-based approaches for the treatment of IVD degeneration.

Acknowledgements

The study was funded by the Italian Ministry of Health, "Ricerca Corrente". S.C. is a PhD supported by grants from the Italian Ministry of Health (Ricerca Corrente). The authors declare no conflict of interest.

References

Bendtsen M, Bunger C, Colombier P, Le Visage C, Roberts S, Sakai D, Urban JPG (2016) Biological challenges for regeneration of the degenerated disc using cellular therapies. Acta Orthop **87**: 39-46.

Bendtsen M, Bunger CE, Zou XN, Foldager C, Jorgensen HS (2011) Autologous stem cell therapy maintains vertebral blood flow and contrast diffusion through the endplate in experimental intervertebral disc degeneration. Spine **36**: E373-E379.

Blanco JF, Graciani IF, Sanchez-Guijo FM, Muntion S, Hernandez-Campo P, Santamaria C, Carrancio S, Barbado MV, Cruz G, Gutierrez-Cosio S, Herrero C, San Miguel JF, Brinon JG, del Canizo MC (2010) Isolation and characterization of mesenchymal stromal cells from human degenerated nucleus pulposus: comparison with bone marrow mesenchymal stromal cells from the same subjects. Spine (Phila Pa 1976) **35**: 2259-2265.

Brisby H, Papadimitriou N, Brantsing C, Bergh P, Lindahl A, Barreto Henriksson H (2013) The presence of local mesenchymal progenitor cells in human degenerated intervertebral discs and possibilities to influence these *in vitro*: a descriptive study in humans. Stem Cells Dev **22**: 804-814.

Brown S, Matta A, Erwin M, Roberts S, Gruber HE, Hanley EN Jr, Little CB, Melrose J (2018) Cell clusters are indicative of stem cell activity in the degenerate intervertebral disc: can their properties be manipulated to improve intrinsic repair of the disc? Stem Cells Dev **27**: 147-165.

Colombini A, Lanteri P, Lombardi G, Grasso D, Recordati C, Lovi A, Banfi G, Bassani R, Brayda-Bruno M (2012) Metabolic effects of vitamin D active metabolites in monolayer and micromass cultures of nucleus pulposus and annulus fibrosus cells isolated from human intervertebral disc. Int J Biochem Cell Biol **44**: 1019-1030.

Colombini A, Lombardi G, Corsi MM, Banfi G (2008) Pathophysiology of the human intervertebral disc. Int J Biochem Cell Biol **40**: 837-842.

Colombini A, Lopa S, Ceriani C, Lovati AB, Croiset SJ, Di Giancamillo A, Lombardi G, Banfi G, Moretti M (2015) *In vitro* characterization and *in vivo* behavior of

human nucleus pulposus and annulus fibrosus cells in clinical-grade fibrin and collagen-enriched fibrin gels. Tissue Eng Part A **21**: 793-802.

de Girolamo L, Lopa S, Arrigoni E, Sartori MF, Preis FWB, Brini AT (2009) Human adipose-derived stem cells isolated from young and elderly women: their differentiation potential and scaffold interaction during *in vitro* osteoblastic differentiation. Cytotherapy **11**: 793-803.

De Luca P, Kouroupis D, Vigano M, Perucca-Orfei C, Kaplan L, Zagra L, de Girolamo L, Correa D, Colombini A (2019) Human diseased articular cartilage contains a mesenchymal stem cell-like population of chondroprogenitors with strong immunomodulatory responses. J Clin Med **8**. pii: E423. DOI: 10.3390/jcm8040423.

Dominici M, Le Blanc K, Mueller I, Slaper-Cortenbach I, Marini F, Krause D, Deans R, Keating A, Prockop D, Horwitz E (2006) Minimal criteria for defining multipotent mesenchymal stromal cells. The International Society for Cellular Therapy position statement. Cytotherapy **8**: 315-317.

Gruber HE, Riley FE, Hoelscher GL, Ingram JA, Bullock L, Hanley EN Jr (2016) Human annulus progenitor cells: analyses of this viable endogenous cell population. J Orthop Res **34**: 1351-1360.

Huang B, Liu LT, Li CQ, Zhuang Y, Luo G, Hu SY, Zhou Y (2012) Study to determine the presence of progenitor cells in the degenerated human cartilage endplates. Eur Spine J **21**: 613-622.

Jackson AR, Huang CY, Gu WY (2011) Effect of endplate calcification and mechanical deformation on the distribution of glucose in intervertebral disc: a 3D finite element study. Comput Methods Biomech Biomed Engin **14**: 195-204.

Keyes WM, Mills AA (2006) p63: a new link between senescence and aging. Cell Cycle **5**: 260-265.

Lee HJ, Choi BH, Min BH, Park SR (2009) Changes in surface markers of human mesenchymal stem cells during the chondrogenic differentiation and dedifferentiation processes *in vitro*. Arthritis Rheum **60**: 2325-2332.

Liu LT, Huang B, Li CQ, Zhuang Y, Wang J, Zhou Y (2011) Characteristics of stem cells derived from the degenerated human intervertebral disc cartilage endplate. PLoS One **6**: e26285. DOI: 10.1371/journal.pone.0026285.

Lopa S, Ceriani C, Cecchinato R, Zagra L, Moretti M, Colombini A (2016) Stability of housekeeping genes in human intervertebral disc, endplate and articular cartilage cells in multiple conditions for reliable transcriptional analysis. Eur Cell Mater **31**: 395-406.

Lopa S, Colombini A, Stanco D, de Girolamo L, Sansone V, Moretti M (2014) Donor-matched mesenchymal stem cells from knee infrapatellar and subcutaneous adipose tissue of osteoarthritic donors display differential chondrogenic and osteogenic commitment. Eur Cell Mater **27**: 298-311.

Lyu FJ, Cheung KM, Zheng Z, Wang H, Sakai D, Leung VY (2019) IVD progenitor cells: a new horizon for understanding disc homeostasis and repair. Nat Rev Rheumatol **15**: 102-112.

Nguyen C, Poiraudeau S, Rannou F (2012) Vertebral subchondral bone. Osteoporos Int **23** Suppl 8: S857-860.

Pattappa G, Li Z, Peroglio M, Wismer N, Alini M, Grad S (2012) Diversity of intervertebral disc cells: phenotype and function. J Anat **221**: 480-496.

Pettine K, Suzuki R, Sand T, Murphy M (2016) Treatment of discogenic back pain with autologous bone marrow concentrate injection with minimum two year follow-up. Int Orthop **40**: 135-140.

Pettine KA, Murphy MB, Suzuki RK, Sand TT (2015) Percutaneous injection of autologous bone marrow concentrate cells significantly reduces lumbar discogenic pain through 12 months. Stem Cells **33**: 146-156.

Pettine KA, Suzuki RK, Sand TT, Murphy MB (2017) Autologous bone marrow concentrate intradiscal injection for the treatment of degenerative disc disease with three-year follow-up. Int Orthop **41**: 2097-2103.

Power KA, Grad S, Rutges JP, Creemers LB, van Rijen MH, O'Gaora P, Wall JG, Alini M, Pandit A, Gallagher WM (2011) Identification of cell surface-specific markers to target human nucleus pulposus cells: expression of carbonic anhydrase XII varies with age and degeneration. Arthritis Rheum **63**: 3876-3886.

Rodrigues-Pinto R, Berry A, Piper-Hanley K, Hanley N, Richardson SM, Hoyland JA (2016) Spatiotemporal analysis of putative notochordal cell markers reveals CD24 and keratins 8, 18, and 19 as notochord-specific markers during early human intervertebral disc development. J Orthop Res **34**: 1327-1340.

Rodrigues-Pinto R, Ward L, Humphreys M, Zeef LAH, Berry A, Hanley KP, Hanley N, Richardson SM, Hoyland JA (2018) Human notochordal cell transcriptome unveils potential regulators of cell function in the developing intervertebral disc. Sci Rep **8**: 12866. DOI: 10.1038/s41598-018-31172-4.

Rutges J, Creemers LB, Dhert W, Milz S, Sakai D, Mochida J, Alini M, Grad S (2010) Variations in gene and protein expression in human nucleus pulposus in comparison to annulus fibrosus and cartilage cells: potential associations with aging and degeneration. Osteoarthritis Cartilage **18**: 416-423.

Sakai D, Grad S (2015) Advancing the cellular and molecular therapy for intervertebral disc disease. Adv Drug Deliv Rev **84**: 159-171.

Sakai D, Nakamura Y, Nakai T, Mishima T, Kato S, Grad S, Alini M, Risbud MV, Chan D, Cheah KS, Yamamura K, Masuda K, Okano H, Ando K, Mochida J (2012) Exhaustion of nucleus pulposus progenitor cells with ageing and degeneration of the intervertebral disc. Nat Commun **3**: 1264. DOI: 10.1038/ncomms2226.

Schol J, Sakai D (2019) Cell therapy for intervertebral disc herniation and degenerative disc disease: clinical trials. Int Orthop **43**: 1011-1025.

Schroeder A, Mueller O, Stocker S, Salowsky R, Leiber M, Gassmann M, Lightfoot S, Menzel W, Granzow M, Ragg T (2006) The RIN: an RNA integrity number for assigning integrity values to RNA measurements. BMC Mol Biol **7**: 3. DOI: 10.1186/1471-2199-7-3.

Schubert AK, Smink JJ, Arp M, Ringe J, Hegewald AA, Sittinger M (2018) Quality assessment of surgical disc samples discriminates human annulus fibrosus and nucleus pulposus on tissue and molecular level. Int J Mol Sci **19**. DOI: 10.3390/ijms19061761.

Urban JP, Smith S, Fairbank JC (2004) Nutrition of the intervertebral disc. Spine (Phila Pa 1976) **29**: 2700-2709.

Wang H, Zhou Y, Huang B, Liu LT, Liu MH, Wang J, Li CQ, Zhang ZF, Chu TW, Xiong CJ (2014) Utilization of stem cells in alginate for nucleus pulposus tissue engineering. Tissue Eng Part A **20**: 908-920.

Web Reference

1. https://earray.chem.agilent.com/earray/ [03-02-2020]

Discussion with Reviewers

Cornelia Neidlinger-Wilke: In the present study, cells isolated from different tissue regions were characterised after *in vitro* expansion in monolayer. Do you think that this had an influence on the outcome of the study? Could you please comment on this possible drawback of the study? Could this influence the conclusion that AF cells might be the best suitable cell population for regenerative purposes? The monolayer culture system is certainly better suitable for AFCs than for NPCs or EPCs. Could you please comment on this?
Authors: Cellular phenotype and surface markers might be altered by *in vitro* dedifferentiation in monolayer, especially if the cells have a more chondrogenic phenotype, such as EPCs and NPCs. The maintenance of cells in monolayer culture for several passages allows for the expansion of the cell population to have a sufficient amount for cell therapy. IVD, as well as cartilaginous EP from adult pathological subjects are low cellularised tissues and, to consider them as sources for cell therapy of degenerative disc disease, few passages in culture of the isolated cells are mandatory. Being not a physiological condition, cell expansion in monolayer may cause alterations to the cell phenotype, especially in NPCs and EPCs. Nevertheless, in this condition, AFCs showed a MSCs-like profile and appeared as the most promising source of tissue-specific cells to be used for the treatment of IVD degeneration.

Sibylle Grad: The authors concluded that expanded AFCs may be a promising source for IVD degeneration cell therapy. Thereby, the expansion conditions may also influence the cellular phenotype. Can the authors comment on the present expansion conditions, potential modifications and their applicability in a (pre-) clinical setting?
Authors: AFCs appeared as the ones having a more promising phenotype after a small number of passages in monolayer. In general, when cultured in monolayer, disc cells tend to lose their tissue-specific phenotype, especially the peculiar matrix proteins and collagen types. To help the cells maintaining their physiological features, 3D cultures, such as in alginate beads, could be considered, although associated with a loss of proliferation. Since a large number of cells is needed for cell therapy, cultivating cells on coated 2D surfaces or addition of growth factors or platelet lysate in the culture media could help to obtain a desirable number of exploitable cells in pre-clinical setting. In the present study, standard culture conditions have been used without addition of any previously mentioned supplement or culture plastic surface coating. Consequently, all the potential strategies above suggested to improve cell products to be exploited for cell therapy will need to be thoroughly tested and validated *in vitro*.

Sibylle Grad: Would the envisaged cell therapy particularly be applicable for AF rupture repair such as after IVD herniation?
Authors: The AF presents a structural complexity and a peculiar biomechanical function that are challenging to restore after rupture. In case of a complete IVD herniation, the anatomical tissue is probably too compromised to allow for the success of a cell therapy approach, even if associated with engineered materials aimed to seal defects in the IVD and, thus, avoid the recurrence of herniation as well as promote cell engraftment. Therefore, the envisaged cell therapy could be applicable for early phase IVD degeneration, in absence of a definitive AF rupture with extrusion of nuclear material and in association with materials able to withstand the mechanical load experienced by the IVD.

Editor's note: The Scientific Editor responsible for this paper was Mauro Alini.